# Todo list



# Simulation and characterization of integrated optics beam combiners for astrointerferometry

I. Physikalisches Institut
Universität zu Köln

*Author :*
Thomas Poletti
M1 Physics and NanoSciences
School-year 2017-2018

*Supervisor:*
Pr. Dr. Lucas Labadie
labadie@ph1.uni-koeln.de

**Abstract**

abstract-text

**Résumé**

Résumé ici

# Contents



# List of Figures



# List of Tables

**Introduction**

Since antiquity and down to our time, astronomers always tried to see further and further in space requiring more and more sensitive instruments. Increasing the telescope diameter is one way to reach higher angular resolution but in the same time make it more sensitive to atmospheric turbulence. Therefore even with the recent progress in adaptative optics, today's largest telescopes can only can only resolve few of the brightest and nearest stars.

Using individual telescopes to form an interferometer, the resolution is determined by the distance between the telescopes. Until recently the instruments combining the light from individual telescopes were bases on costly and cumbersome bulk optics. The recent advances in manufacturing integrated-optics and especially in laser processing have resulted in new instruments that are operational on sky and delivering higher quality results.

The purpose of this work is to optimise and characterise the performance of Integrated optic (IO) beam combiners and especially one promising type of component called discrete beam combiner (DBC). Allowing to retrieve the astronomical parameters without scanning the interferogram these components could allow to observe fast varying objects.

This report is organised in three parts. In the first part I will present the motivation and the basis of astronomical interferometry. In the second part will be presented the simulation results of the DBC as well as its optimisation. In the last part will be discussed the experimental characterisation of asymmetric couplers, Multi Mode Interferometer (MMI) and of the DBC.

# 1 Motivation and scientific background

- quoi quest-ce linterferometrie, intérêt par rapport à lobservation par un télescope mono-pupille en terme de résolution angulaire - nulling, contraintes - schema hi-5, explications - VLTI - bandes dobservation - unités astro - Bases de la BeamPropMethod

# 2 Simulation of the DBC

The discrete beam combiner is a component made of multiple straight waveguides close to each other. It has been demonstrated that in the case of a $N$ telescope DBC, an array of more than $N^2$ waveguides is needed for efficient operation of the DBC [Min12]. But at this point is hasn't been studied the impact of other geometrical parameters such as the spacing between each waveguides.

The component studied is formed of 23 outputs and four inputs to combine the light from four individual telescopes. A cross-section of it is shown on Fig. 1. Both the input configuration and the "Zig-Zag" shape have already been optimised. After a brief explanation of the theory behind the DBC we will focus on optimising it regarding $P_x$,

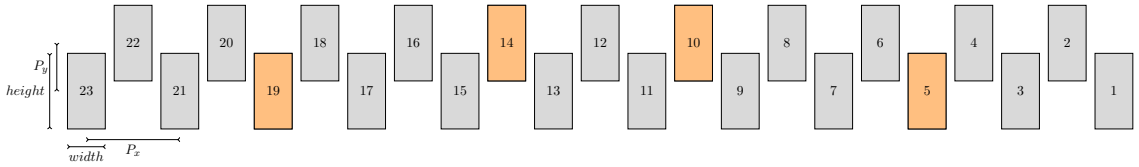


Figure 1: The Zig-Zag array's cross section with the numbering convention. The four input waveguides are displayed in orange.

$P_y$, *width*, *height* and the length of the DBC part (the notations refers to Fig. 1) in the case of monochromatic light. In a second part the performances of the optimised component regarding the bandwidth of the input light are simulated. All simulation are performed using the commercial software Beamprop in scalar mode (a full-vectorial mode would have been more accurate but didn't show much different results for both TE and TM polarisation regarding the condition number of the Visibility to Pixel Matrix (V2PM) -see next section-), correlation mode and transparent boundary condition. The grid size was chosen as a balance between computation time and accuracy.

## 2.1 Monochromatic light

In this section is shown the impact on the performances of the DBC regarding its geometry. Two main parameters are studied, the condition number of the V2PM and the throughput as it hadn't been done before.

### 2.1.1 Mathematical formalism

As stated before the "Zig-Zag" DBC is composed of 23 outputs and can combine the light from 4 individual telescopes. This component has the particularity that all the information about the coherence function of the studied object is included in the way the 23 outputs are related to each other [TMC+07]. In the case of monochromatic light the theory is exact. We will do a brief overview of the theoretical background in this part. For further reading the reader can refer to [TMC+07, SMD+13, DTL+17].

In this part we will consider the light combined from the input $A$ and $B$ at the $n^{th}$ output. In that case the intensity $I_n$ at the output can be expresed as :

$$I_n = \kappa_A I_A + \kappa_B I_B + 2\sqrt{\kappa_A I_A \kappa_B I_B} V_{AB}^{inst} V_{AB}^{obj} \cos(\phi_{AB}^{inst} + \phi_{AB}^{obj}) \quad (1)$$

In this equation $\kappa_i$ is the transmission coefficient from the input $i$ to the considered output. *inst* and *obj* relates the visibility/phases of the instrument and of the observed object. Equation 1 can easily be reduced to Eq.2 in which the produce of the instrumental and object visibility are reduced in $V_{AB}$.

$$I_n = \kappa_A I_A + \kappa_B I_B + 2\sqrt{\kappa_A I_A \kappa_B I_B} V_{AB} \left( \cos(\phi_{AB}^{inst}) \cos(\phi_{AB}^{obj}) - \sin(\phi_{AB}^{inst}) \sin(\phi_{AB}^{obj}) \right) \quad (2)$$

From Eq.2 the problem of getting the object mutual coherence function can be reduced to the produce of a matrix and a vector. Thus the characteristics of the input fields can be linked to the output intensities by the relation :

$$\vec{I} = V2PM \times \vec{V} \quad (3)$$

In which $\vec{I} = (I_1, ...I_M)^T$ represent the intensities at the M outputs,
$\vec{V} = (I_1, ..., I_M, V_{12}^{obj}\sqrt{I_1 I_2} cos(\Phi_{21}^{obj}), V_{12}^{obj}\sqrt{I_1 I_2} sin(\Phi_{21}^{obj}), ..., V_{N-1,N}^{obj}\sqrt{I_{N-1} I_N} cos(\Phi_{N,(N-1)}^{obj}), V_{N-1,N}^{obj}\sqrt{I_{N-1} I_N} sin(\Phi_{N,(N-1)}^{obj}))$
and the visibility to pixel matrix V2PM represent the beam combiner's properties. An example of a V2PM for an hypothetical beam combiner with 3 inputs and 2 outputs is displayed in Figure 2

$$\begin{pmatrix} \kappa_{11} & \kappa_{21} & \kappa_{31} & 2V_{12}^1\sqrt{\kappa_{11}\kappa_{21}} cos(\Phi_{12}^{inst}) & -2V_{12}^1\sqrt{\kappa_{11}\kappa_{21}} sin(\Phi_{12}^{inst}) & 2V_{13}^1\sqrt{\kappa_{11}\kappa_{31}} cos(\Phi_{13}^{inst}) & -2V_{13}^1\sqrt{\kappa_{11}\kappa_{31}} sin(\Phi_{13}^{inst}) & 2V_{23}^1\sqrt{\kappa_{21}\kappa_{31}} cos(\Phi_{23}^{inst}) & -2V_{23}^1\sqrt{\kappa_{21}\kappa_{31}} sin(\Phi_{23}^{inst}) \\ \kappa_{12} & \kappa_{22} & \kappa_{32} & 2V_{12}^2\sqrt{\kappa_{12}\kappa_{22}} cos(\Phi_{12}^{inst}) & -2V_{12}^2\sqrt{\kappa_{12}\kappa_{22}} sin(\Phi_{12}^{inst}) & 2V_{13}^2\sqrt{\kappa_{12}\kappa_{32}} cos(\Phi_{13}^{inst}) & -2V_{13}^2\sqrt{\kappa_{12}\kappa_{32}} sin(\Phi_{13}^{inst}) & 2V_{23}^2\sqrt{\kappa_{22}\kappa_{32}} cos(\Phi_{23}^{inst}) & -2V_{23}^2\sqrt{\kappa_{22}\kappa_{32}} sin(\Phi_{23}^{inst}) \end{pmatrix}$$

Figure 2: An hypothetical V2PM matrix for a 3 to 2 beam combiner. All visibility and phases in the matrix are the instrumental ones.

One can find the pixel to visibility matrix by inverting the V2PM matrix with the relation 4 and then the astronomical information from $\vec{V}$. To be consistent with the notation introduced in [SMD+13], $\vec{V} = (\Gamma_{11}, ..., \Gamma_{MM}, \mathcal{R}\Gamma_{12}, \mathcal{I}\Gamma_{12}, ..., \mathcal{R}\Gamma_{N(N-1)}, \mathcal{I}\Gamma_{N(N-1)})$ the object phase and visibility can be extracted by :

$$V_{ij}^{obj} = \sqrt{\frac{(\mathcal{R}\Gamma_{ij})^2 + (\mathcal{I}\Gamma_{ij})^2}{\Gamma_{ii}\Gamma_{jj}}} \qquad \Phi_{ij}^{obj} = arctan(\frac{\mathcal{I}\Gamma_{ij}}{\mathcal{R}\Gamma_{ij}}) \quad i \neq j$$

$$P2VM = (V2PM^T \times V2PM)^{-1} \times V2PM^T \quad (4)$$

In the light of this formalism the retrieved coherence function from the Pixel to Visibility Matrix (P2VM) can be inaccurate and one has to minimize the condition number of the matrix in order to minimize the possibility of a strong amplification of measure inaccuracy. For further explanation on this subject refers to Annexe A.1

### 2.1.2 Impact of evanescent coupling on the output power

Firstly it is important to understand how much the way chosen to calculate the power at an output could affect the phases relations and visibilities. This part present the impact

of the surface over which is calculated the power on the resulting phases relations and visibilities.

Considering only 3 distinct wave-guides of the DBC Zig-Zag component. The cross section of each WG is a rectangle $width \times height$. In such a dielectric wave-guide, there is no analytical solution to the scalar wave equation but according to [Lab08] a good approximation of the transverse field profile is close to a gaussian :

$$\Psi(x,y) \approx \Psi_0 exp\left(\frac{-x^2}{\omega_x^2} + \frac{-y^2}{\omega_y^2}\right)$$

Using this equation and retrieving $\omega_x$ and $\omega_y$ from BeamProp simulation by the width of the gaussian at $1/e$ of its maximal amplitude, we can «calculate» the transverse field profile in the wave-guide.

We simulate this behaviour for the following parameters (in µm) :

- Px =24
- Py = 10.8
- width = 9.5
- height = 17
- $n_{clad} = 2.31$
- $\delta n = 0.005$

In this case we have $\omega_x \approx 7.798$ and $\omega_y \approx 10.114$. The resulting field for 3 outputs in phase and guiding the same power is shown in Fig. 3.

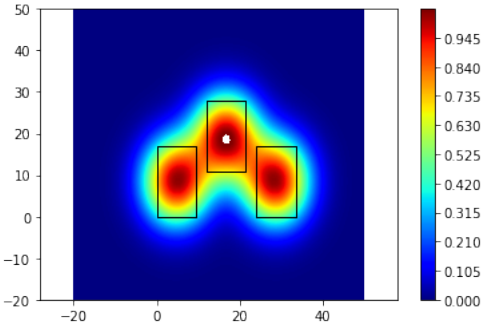


Figure 3: Example of 3 outputs in phase guiding the same power. The modes are Gaussian perfectly centred on the wave-guide

One can see that in this case, where the 3 outputs are in phase, the determination of the power in the middle WG will be badly estimated by a simple power integral as :

$$P \propto \iint_{\mathbb{R}^2} \Psi^*(x,y)\Psi_{sim}(x,y)dxdy \tag{5}$$

where $\Psi_{sim}$ is the simulated output fields as shown on the upper figure. Therefore the integration should be limited to a user-defined area around the WG. In the next paragraph we try to have a first feeling of the impact of this choice on the phases relations, instrumental visibilities and of course the V2PM matrix.

**Power of a Gaussian field :** For an isolated gaussian field the power $P$ is given by

$$\frac{P}{\Psi_0^2} \propto \iint_{\mathbb{R}^2} exp\left(\frac{-2x^2}{\omega_x^2} + \frac{-2y^2}{\omega_y^2}\right) dxdy = \frac{\pi}{2}\omega_x\omega_y$$

In the case of our parameters it is equal to 123.88 µm$^2$ (a numerical integration using the composite trapezoidal rule lead to 123.76). By integrating the whole field as represented in Fig. 3 we obtain 113.70 µm$^2$ but the truly guided power in the central wave-guide calculated over the cross-section should only be 87.39 µm$^2$ thus an error of 30 %.
In the opposite case where there is no power in the central wave-guide, and a maximal power in the two surrounding wave-guides we find a guided power in the central wave-guide over the cross-section of 3.10 µm$^2$. It can easily be understood that the simulated (ergo the experimental) interferograms will depend of the considered area. The larger this area, the greater the impact of the surrounding wave-guides on the interferogram.

**Influence on the simulated phases relations :** We have seen that the integrating area used to estimate the guided power should have a great impact on the result, we now try to see its impact on the simulated phase relations. To do this the 3 gaussian are multiplied by a cosine to simulate a phase dependency. The left and right outputs are set with phases pi/3 and 2pi/3 respectively and the middle one with phase 0. The power is then integrated on different area centred the WG cross-section.

One can see that in this case, the phase of the output signal is mostly unchanged by the integrating area, but this is only the case for area slightly larger to the WG's cross section. Therefore it might be expected that the phase relation between outputs with comparable power magnitude will stay the same for low variation of the integrating area. The only changed parameter might be the Visibilities but one can not conclude as the mean value, ergo the photometries changes too.

To this point we have only seen the impact of the integrating area when all outputs are guiding the same maximal power. It is now studied the impact on a low guided power in the middle WG comparatively to the left and right ones. Same phases are introduced. The power in the left and right WG are the same and 4 times the power in the middle WG. The results to those simulations are shown in Fig. 4

As can be seen, the more the power difference between the middle WG and the sides WG and the larger the integrating area, the more impacted the retrieved phase differences. Therefore it seems that the V2PM matrix of the component should be calculated not only for the isolated component but also with the imaging system. One way to get rid of these

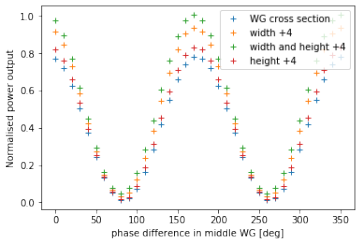


(a) Simulation with the same power in the middle and the surroundings WG.

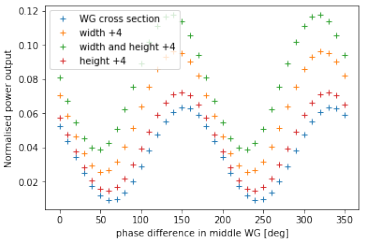


(b) Simulation with low power in the middle WG and high in the surroundings.

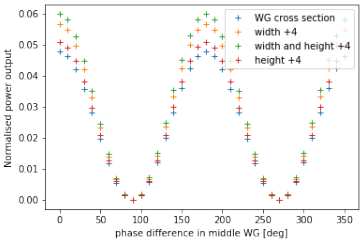


(c) Simulation with low power in the middle WG and high in the surroundings for a higher x spacing between the WG.

Figure 4: Influence of different parameters on the phases and amplitudes of the interferogram in the middle wave-guide. The phases relations between the outputs are highly influenced by the evanescent coupling

dependency would be to have a greater spacing between the WG at the output so that the evanescent coupling is as low as possible (as shown in Fig. 4c). Thus the use of a «fan out» could be an option to have calculate the power over a larger area thus have a greater integrated power (ergo a smaller signal to noise ratio (SNR)).

#### 2.1.3 Influence of geometrical parameters

#### 2.1.4 Retrieving the visibility function

### 2.2 Polychromatic light

#### 2.2.1 Mathematical formalism

#### 2.2.2 Influence of the bandwidth

#### 2.2.3 Retrieving the visibility function

## 3 Laboratory characterization of beam combiners

### 3.1 Asymmetric couplers

### 3.2 MMI

### 3.3 Discrete Beam Combiner

## Conclusion and Further-work

# A Appendix

## A.1 The condition number

Considering the following system $A\vec{x} = \vec{b}$ where A is the matrix describing our system (A is a matrix with real coefficients). An error $\vec{\delta x}$ on $\vec{x}$ will lead to an error $\vec{\delta b}$ on $\vec{b}$. The aim is to know how much bigger or smaller is $\frac{\left\|\vec{\delta x}\right\|}{\|\vec{x}\|}$ compared to $\frac{\left\|\vec{\delta b}\right\|}{\left\|\vec{b}\right\|}$ (i.e how much an error is magnified by the A matrix).

In the case where A in neither symmetric nor square. Then the matrix $A^T A$ is a square symmetric matrix and Then can be diagonalized. Lets call $\lambda_i$ and $\vec{u_i}$ its eigenvalues and eigenvectors. We can write :

$$A^T A\vec{u_i} = \lambda_i \vec{u_i}$$

Moreover

$$\|A\vec{x}\|^2 = \vec{x}^T A^T A\vec{x} = \left\|\vec{b}\right\|^2$$

So $\left\|\vec{b}\right\|^2 \leq max(|\lambda_i|)\,\|\vec{x}\|^2$ and $\left\|\vec{\delta b}\right\|^2 \geq min(|\lambda_i|)\left\|\vec{\delta x}\right\|^2$ and then :

$$\boxed{\frac{\left\|\vec{\delta x}\right\|}{\|\vec{x}\|} \leq \frac{\sqrt{max(|\lambda_i|)}}{\sqrt{min(|\lambda_i|)}}\frac{\left\|\vec{\delta b}\right\|}{\left\|\vec{b}\right\|}}$$

The number $\frac{\sqrt{max(|\lambda_i|)}}{\sqrt{min(|\lambda_i|)}}$ where $min(|\lambda_i|)$ is the minimal non zero eigenvalue of $A^T A$, is called the condition number of the A matrix. It means how much an error on the right part of the system can be magnified by the A matrix.

# Glossary

**DBC** discrete beam combiner. 1, 2

**IO** Integrated optic. 1

**MMI** Multi Mode Interferometer. 1

**V2PM** Visibility to Pixel Matrix. 2

## Bibliography

[DTL+17] Romina Diener, Jan Tepper, Lucas Labadie, Thomas Pertsch, Stefan Nolte, and Stefano Minardi. Towards 3d-photonic, multi-telescope beam combiners for mid-infrared astrointerferometry. 25:19262, 08 2017.

[Lab08] Pierre Labeye. *Integrated optics components for stellar interferometry*. Theses, Institut National Polytechnique de Grenoble - INPG, February 2008.

[Min12] S. Minardi. Photonic lattices for astronomical interferometry. *Monthly Notices of the Royal Astronomical Society*, 422(3):2656–2660, 2012.

[SMD+13] Allar Saviauk, Stefano Minardi, Felix Dreisow, Stefan Nolte, and Thomas Pertsch. 3d-integrated optics component for astronomical spectro-interferometry. 52:4556–4565, 07 2013.

[TMC+07] Eric Tatulli, F Millour, A Chelli, Gilles Duvert, Bram Acke, Oscar Hernandez Utrera, K H. Hofmann, S Kraus, Fabien Malbet, Mege Pierre, Romain Petrov, Michael Vannier, Gerard Zins, P Antonelli, Udo Beckmann, Y Bresson, Michel Dugue, S Gennari, L Glück, and Noemi Ventura. Interferometric data reduction with amber/vlti. principle, estimators, and illustration. 464, 03 2007.